

# Unsteady power coefficient evolution in a Savonius wind turbine

*Jihen Marzougui*<sup>1\*</sup>, *Nour Rabeh*<sup>1</sup>, *Ahmed Ayadi*<sup>2</sup>, and *Ridha Ennetta*<sup>1,2</sup>

<sup>1</sup> Laboratory of Mechanical Modeling, Energy & Materials (LM2EM), National Engineering School of Gabes (ENIG), University of Gabes, Tunisia

<sup>2</sup> Higher Institute of Industrial Systems of Gabes (ISSIG), University of Gabes, Tunisia

**Abstract.** Wind energy is an attractive solution for small-scale and urban applications, particularly in low-wind environments where horizontal-axis turbines are less efficient. In this context, drag-based vertical axis wind turbines (VAWTs), especially the Savonius rotor, offer advantages such as simple construction, low cost, omnidirectional operation, and strong self-starting capability. However, their relatively low aerodynamic efficiency requires accurate performance evaluation. This study analyzes the evolution of the power coefficient ( $C_p$ ) over successive rotor revolutions at different tip speed ratios (TSR) using unsteady numerical simulations. The objective is to distinguish transient startup effects from steady state behavior. Results indicate the presence of an initial transient phase, during which  $C_p$  progressively increases as the flow develops around the rotor. After several revolutions, the turbine reaches a quasi-steady regime where  $C_p$  variations become minimal and periodic. These findings demonstrate that reliable performance assessment must be conducted only after transient effects have dissipated. Considering unsteady aerodynamic behavior is therefore essential for accurate evaluation and effective optimization of Savonius rotor performance.

## 1 Introduction

The Savonius turbine is a drag-driven vertical axis wind turbine (VAWT) known for its simple structure [1], self-starting capability, and effective operation at low wind speeds. Unlike lift-based turbines, it operates primarily through the difference in drag forces acting on the advancing and returning blades. This mechanism enables omnidirectional wind capture without the need for a yaw system, making the Savonius rotor particularly suitable for decentralized and urban energy applications [2]. CFD simulations help estimate aerodynamic forces, torque, and power extracted by Savonius rotors.

Despite its structural advantages, the aerodynamic performance of the Savonius rotor remains limited by negative torque generation during certain angular positions and by highly unsteady flow characteristics [3]. The interaction between separated flow regions, vortex shedding, and blade motion produces significant torque fluctuations, which directly affect system stability and overall efficiency [4:5]. Various geometric modifications and flow

---

\* Corresponding author: [jihen.marzougui.j@gmail.com](mailto:jihen.marzougui.j@gmail.com)

control strategies have therefore been investigated to mitigate these effects and enhance performance [6:7].

In this chapter, special attention is given to the transient behavior of the rotor by observing the evolution of the power coefficient ( $C_p$ ) over ten consecutive rotations. Monitoring  $C_p$  across multiple cycles allows for a clearer understanding of performance stabilization, periodicity, and convergence characteristics. The main objective is to analyze how the aerodynamic performance develops with time and to determine whether the rotor reaches a quasi-steady operational regime after several rotations. This approach provides deeper insight into the dynamic response and overall efficiency of the Savonius rotor.

## 2 Methods and materials

### 2.1 Geometry of savonius rotor

The Savonius rotor investigated in this study consists of two semi-cylindrical blades, as shown in Figure 1, and follows the experimental configuration reported by Sheldahl et al. [8]. The rotor diameter ( $D$ ) is 0.909 m, with a blade-to-rotor diameter ratio ( $d/D$ ) of 0.55. The rotating computational domain is defined as 1.1 times the rotor diameter to ensure accurate representation of the surrounding flow field.

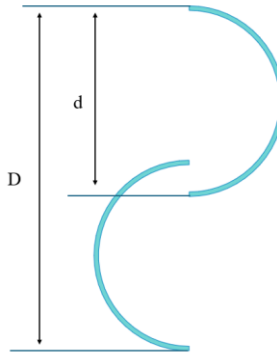


**Fig. 1.** Geometrical schematic of a standard semi-cylindrical Savonius rotor design.

### 2.2 Computational setup

#### 2.2.1. Boundary conditions

The flow around the Savonius wind rotor is simulated using ANSYS Fluent to study its turbulent characteristics. Based on previous research, the  $k-\omega$  SST turbulence model has been shown to reliably predict rotor performance and capture flow separation phenomena [9,10]. As shown in Figure 2, the computational domain consists of a rotating zone containing the rotor blades, surrounded by a stationary outer region. A uniform inflow velocity of 7 m/s was applied. The outlet was set to atmospheric pressure, while symmetry conditions were enforced on the top and bottom boundaries [11].

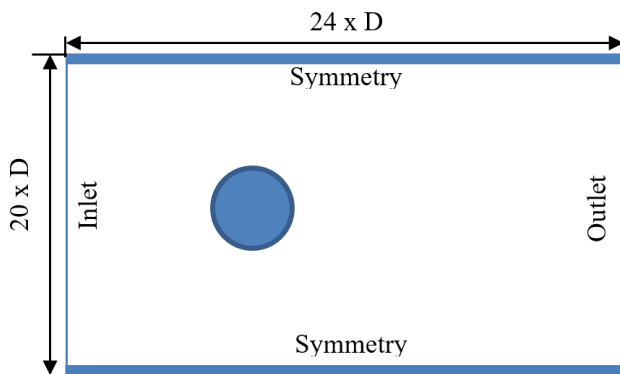


**Fig. 2.** Boundary conditions.

### 2.2.2. Meshing

Using ANSYS Workbench, an unstructured predominantly quadrilateral mesh was generated for the entire computational domain. A finer mesh was applied within the rotating zone to better capture blade aerodynamics, while the stationary region used a comparatively coarser grid. To accurately resolve boundary layer effects, twenty inflation layers with a specified growth rate of 1.1 were implemented along the blade surfaces. Additional refinement was introduced at the rotating stationary interface to ensure geometric consistency. Since finer meshes increase computational cost, a mesh independence study was performed.

In this present study, three different mesh densities were examined to evaluate grid sensitivity, such as, coarse (92,907 nodes), medium (109,858 nodes), and fine (147,531 nodes). The results showed strong agreement between the medium and fine mesh cases, indicating that further refinement did not produce noticeable changes in the predicted performance. Consequently, the mesh containing 109858 elements was particular for subsequent simulations, ensuring a balanced approach to processing cost and result accuracy.

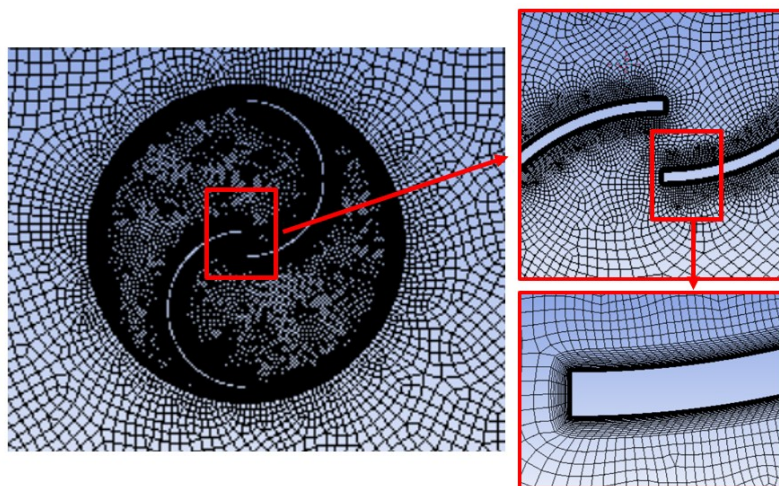


**Fig. 3.** Refined mesh configuration in the vicinity of the Savonius turbine blade.

### 2.3 Numerical model validation

The numerical model was verified by simulating a standard Savonius rotor and comparing the outcomes with experimental data [8]. As shown in Figure 4, the results closely match earlier numerical studies, demonstrating the accuracy and dependability of the current simulations.

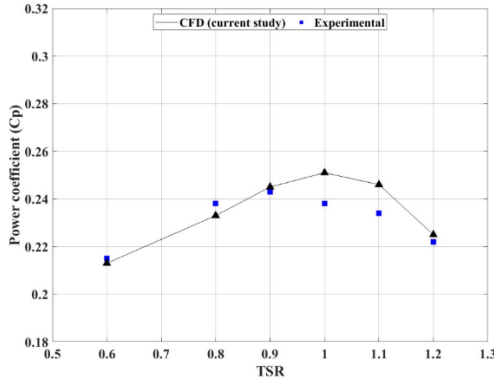


Fig. 4. Experimental results versus numerical simulation outcomes

## 3 Results

### 3.1 Instantaneous torque variation

Figure 5 depicts how the torque coefficient ( $C_t$ ) changes with the rotation angle over several revolutions of the Savonius rotor obtained from the ANSYS Fluent simulation. The initial stage of the curve represents the transient regime, characterized by significant oscillations and noticeable amplitude fluctuations as the flow field develops and the rotor response stabilizes under the imposed boundary conditions. After approximately  $2160^\circ$  of rotation, the solution reaches a periodic steady state, where both the amplitude and frequency of the oscillations become nearly constant. For accurate performance assessment, the mean torque coefficient was computed over the last complete rotation cycle within the steady region, ensuring that start-up effects were excluded and that the reported value represents the fully developed periodic behavior of the rotor.

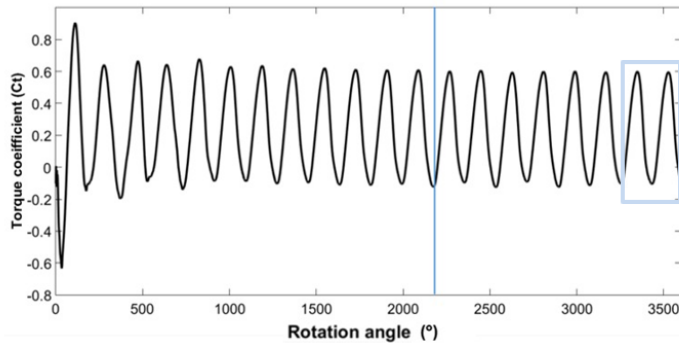
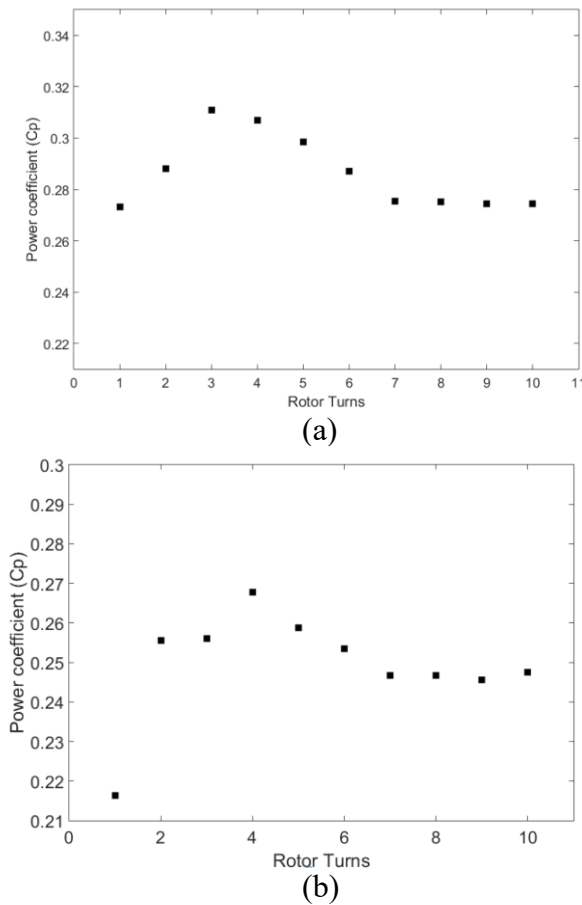


Fig. 5. Torque coefficient evolution as a function of revolution number at  $TSR = 1.1$ .

### 3.2 Average power coefficient

Figure 6 depicts the changes in the power coefficient over the number of rotor revolutions during the simulation of a VAWT equipped with a Savonius-type rotor at (a)  $TSR = 1$  and (b)  $TSR = 1.1$ . During the initial phase, between the 1st and 6th revolution,  $C_p$  increases significantly, corresponding to the transient period in which the flow around the rotor, characterized by complex vortex shedding and blade wake interactions, is not yet stable. After this stage,  $C_p$  slightly decreases and then fluctuates within a narrow range, with a small difference between its minimum and maximum values. These limited oscillations indicate that the rotor has reached a quasi-steady periodic regime, enabling a reliable evaluation of its aerodynamic performance. The evolution of  $C_p$  over 10 revolutions confirms that this duration is sufficient to capture both the startup transient and the steady-state behavior.



**Fig. 6.** Evolution of power coefficient over rotor turns at (a)  $TSR=1$  (b)  $TSR=1.1$

## 4 Conclusion

This work used unsteady numerical simulations to investigate the transient and steady state performance evaluation of a Savonius vertical axis wind turbine. The evolution of the power coefficient across successive rotor revolutions revealed a substantial transient phase at starting, followed by a quasi-steady periodic regime. The findings verified that  $C_p$  initially

rises as the flow field gradually forms around the rotor, then stabilizes after many rotations when aerodynamic forces become repeatable. The data suggest that evaluating performance based on early rotor cycles may result in misleading efficiency estimates. Reliable assessment should therefore be performed only after the stabilization phase is completed. Overall, this study stresses the need of taking transient aerodynamic effects into account when studying and optimizing Savonius rotor performance. This approach helps to improve the accuracy of numeric

## References

1. A. Ayadi, N. Rabeh, J. Marzougui, R. Ennetta, Z. Driss, Investigation of the blade tip geometry for improved performance of a Savonius rotor. *Results Eng.* 27, 106745 (2025).
2. J. Marzougui, A. Ayadi, N. Rabeh, R. Ennetta, Z. Driss, Enhancing Savonius turbine performance via novel concave-side blade designs. *Environ. Prog. Sustainable Energy* e70236 (2025).
3. W. Tian, X. Ni, Z. Mao, Y.-F. Wang, Study on the performance of a new VAWT with overlapped side-by-side Savonius rotors. *Energy Convers. Manage.* 264, 115746 (2022).
4. Y. Yan, J. Zhang, J. She, W. Liu, J. Deng, J. Zhu, Effect of additional cylinders on power-extraction performance of a Savonius vertical-axis wind turbine. *J. Zhejiang Univ.-Sci. A* 24(6), 531–542 (2023).
5. E. Fatahian, F. Ismail, M.H.H. Ishak, W.S. Chang, Flow dynamics and performance enhancement of drag-type Savonius wind turbine with a novel elliptic-shaped deflector. *Flow Turbul. Combust.* 114(2), 643–675 (2025).
6. A.R. Sengupta, S. Rakshit, H. Majumder, A comprehensive review on various approaches for performance improvement of Savonius wind turbines. *Discov. Appl. Sci.* 8(1), 79 (2025).
7. M. Mohan, U.K. Saha, Computational study of a newly developed parabolic blade profile of a Savonius wind rotor. *J. Braz. Soc. Mech. Sci. Eng.* 45(10), 548 (2023).
8. R.E. Sheldahl, B.F. Blackwell, L.V. Feltz, Wind tunnel performance data for two- and three-bucket Savonius rotors. *J. Energy* 2(3), 160–164 (1978).
9. M. Lajnef et al., Numerical and experimental investigation for helical Savonius rotor performance improvement using novel blade shapes. *Ocean Eng.* 309, 118357 (2024).
10. G. Ferrari, D. Federici, P. Schito, F. Inzoli, R. Mereu, CFD study of Savonius wind turbine: 3D model validation and parametric analysis. *Renew. Energy* 105, 722–734 (2017).
11. M.E. Eshagh Nimvari, H. Fatahian, E. Fatahian, Performance improvement of a Savonius vertical axis wind turbine using a porous deflector. *Energy Convers. Manage.* 220, 113062 (2020).